

FEDSM99-7062

DISCRETE WAVELETS TRANSFORM ANALYSIS IN AXIAL VELOCITY
DISTRIBUTION OF SPIRAL FLOW

Masahiro TAKEI
Nihon University, Tokyo Japan

Yao-Hua ZHAO
University of Tokyo, Tokyo Japan

Yoshifuru SAITO
Hosei University, Tokyo Japan

Hui LI
Kagoshima University, Kagoshima Japan

Mitsuaki OCHI
Nihon University, Tokyo Japan

Kiyoshi HORII
Shirayuri College, Tokyo Japan

ABSTRACT

Time-frequency distributions of axial turbulence velocities of spiral pipe flow and typical turbulence flow have been clearly decomposed in a range from low frequency level to high frequency level by means of discrete wavelets transform. As a result, the lower frequency levels (under Level 4) of the spiral flow are extremely lower as compared with those of the typical turbulence flow. Moreover, the spiral flow is dominated by Level 3 to be stabilized from the autocorrelation. The originality of this paper lies in applying discrete wavelets transform and its autocorrelation analysis to analyzing the spiral flow stable motion in time-frequency dimension.

KEYWORDS Discrete wavelets transform, Spiral flow, Frequency analysis, Turbulence velocity, Fluctuation level, Autocorrelation

INTRODUCTION

Spiral flow is a swirling flow with large free vortex region, high concentration to the axis and high stability [Horii et al. 1990]. From the high stability characteristics, the spiral flow is useful for industrial applications such as optical cord installation in a small diameter pipeline with bends [Horii et al. 1991] and high performance pneumatic transportation without particles touching pipe inner wall [Takei et al. 1997]. The solids in the two-phase spiral pipe flow acquire stably their position in a pipeline without large vibration. The motivation behind this work is to clarify the mechanism of the high stability in order to improve the spiral flow system. Time-frequency analysis is a suitable method to analyze the stability.

Recently, wavelets transform has been popular for time-frequency analysis instead of Fourier transform in mechanical engineering fields. The merits of the wavelets analysis is to be able to analyze the frequency not to erase the time information. Wavelets transform [Moret 1989] is roughly classified with two

types, which are continuous wavelets transform and discrete wavelets transform. The continuous wavelets transform has been generally used for time frequency analysis in vibration wave. For example, self-similarity of the inner structure of the jet [Everson 1990], the breakdown of a large eddy and the successive branching of a large eddy structure in a plane jet [Li 1995], decomposition of Reynolds stress in a jet [Gordeyev 1995], and the multiple acoustic modes and the shear layer instability [Walker 1995] were investigated.

However, most of the researchers on the time-frequency analysis carried out the continuous wavelets transform. On the other hand, the discrete wavelets transform has been mainly used for picture image processing. The analysis enables to decompose and to compose of picture image data quantitatively because of the orthonormal transform. Saito applied this idea to analyzing the electromagnetic wave [Saito 1996].

The originality of this paper lies in applying discrete wavelets transform and autocorrelation to each frequency level to analyzing the spiral flow stable motion. In this paper, as a first step to clarify the stability, time-frequency distribution of axial turbulence velocity of spiral pipe flow is decomposed from low frequency level to high frequency level by discrete wavelets transform and its auto correlation. It is recognized which level is dominant to stabilize the spiral flow.

THEORY OF DISCRETE WAVELETS TRANSFORM
Basic Concept Using Simple Base Function

Basic concept of discrete wavelets transform is described using matrix expression instead of integral expression. One dimensional input data matrix with four elements X and an analyzing wavelets matrix of Haar base function W are used to simplify the expression. For example, the input data matrix X is discrete velocity data with time. The wavelets transform matrix S that indicates wavelets spectrum is expressed by

$$\begin{bmatrix} S_1 \\ D_1 \\ d_1 \\ d_1 \end{bmatrix} = \begin{pmatrix} 1 \\ \sqrt{2} \end{pmatrix} \begin{bmatrix} 1 & 1 & 1 & 1 \\ 1 & 1 & -1 & -1 \\ \sqrt{2} & -\sqrt{2} & 0 & 0 \\ 0 & 0 & \sqrt{2} & -\sqrt{2} \end{bmatrix} \begin{bmatrix} a \\ b \\ c \\ d \end{bmatrix} \quad (1)$$

$$\text{or } S = W \cdot X \quad (2)$$

Where, $W^T \cdot W = I$, I is a unit matrix and W^T is a transpose matrix of W . The analyzing wavelets matrix is an orthonormal. In Eq. (1), the first element in the wavelets spectrum S_1 shows a transform to obtain a mean value with a weight on the all input data, $a+b+c+d$. The second element in the wavelets spectrum D_1 shows a transform to obtain a difference value between the first half and the latter half with a weight on the input data, $(a+b)-(c+d)$. It means that this element includes the lower frequency level of the input data. The third element d_1 shows a transform to obtain a difference value on the first half of the input data, $(a-b)$. The fourth element d_1 is a transform to obtain a difference value on the latter half, $(c-d)$. The third and fourth elements include the higher frequency level of the input data. Therefore, the input data is able to be classified to a range from higher frequency level to lower frequency level. Because of orthonormal, the inverse discrete wavelets transform is expressed by,

$$X = W^T \cdot S \quad (3)$$

Moreover, from Eq. (3), the input data X is decomposed by multiresolution. The matrix expression is

$$\begin{bmatrix} a \\ b \\ c \\ d \end{bmatrix} = \begin{pmatrix} 1 \\ \sqrt{2} \end{pmatrix} \begin{bmatrix} 1 & 1 & \sqrt{2} & 0 \\ 1 & 1 & -\sqrt{2} & 0 \\ 1 & -1 & 0 & \sqrt{2} \\ 1 & -1 & 0 & -\sqrt{2} \end{bmatrix} \begin{bmatrix} S_1 \\ D_1 \\ d_1 \\ d_1 \end{bmatrix} = W^T \begin{bmatrix} S_1 \\ 0 \\ 0 \\ 0 \end{bmatrix} + W^T \begin{bmatrix} 0 \\ D_1 \\ 0 \\ 0 \end{bmatrix} + W^T \begin{bmatrix} 0 \\ 0 \\ d_1 \\ d_1 \end{bmatrix} \quad (4)$$

$$\text{or } X = W^T S = W^T S_0 + W^T S_1 + W^T S_2 \quad (5)$$

Where, $S_0 = [S_1 \ 0 \ 0 \ 0]^T$, $S_1 = [0 \ D_1 \ 0 \ 0]^T$, $S_2 = [0 \ 0 \ d_1 \ d_1]^T$. $W^T S_0$, $W^T S_1$ and $W^T S_2$ are called Level 0, Level 1 and Level 2, respectively.

Generalization of Discrete Wavelets Transform

Many orthonormal wavelets analyzing function are found [Molet 1989]. The basic concept of the discrete wavelets transform is generalized by using fourth Daubechies function (N=4). The analyzing wavelets matrix is also an orthonormal function. The analyzing wavelets matrix W is acquired by a cascade algorithm on the basis of a function matrix C . The matrix C is shown in Eq. (6).

$$C = \begin{pmatrix} c_0 & c_1 & c_2 & c_3 & 0 & 0 & 0 & 0 & 0 & 0 \\ c_1 & -c_2 & c_1 & -c_0 & 0 & 0 & 0 & 0 & 0 & 0 \\ 0 & 0 & c_0 & c_1 & c_2 & c_3 & 0 & 0 & 0 & 0 \\ 0 & 0 & c_1 & -c_2 & c_1 & -c_0 & 0 & 0 & 0 & 0 \\ \dots & \dots & \dots & \dots & \dots & \dots & \dots & \dots & \dots & \dots \\ 0 & 0 & 0 & 0 & 0 & 0 & c_0 & c_1 & c_2 & c_3 \\ 0 & 0 & 0 & 0 & 0 & 0 & c_1 & -c_2 & c_1 & -c_0 \\ c_2 & c_1 & 0 & 0 & 0 & 0 & 0 & 0 & c_0 & c_1 \\ c_1 & -c_2 & 0 & 0 & 0 & 0 & 0 & 0 & c_1 & -c_2 \end{pmatrix} \begin{matrix} c_0 = \frac{1+\sqrt{3}}{4\sqrt{2}} \\ c_1 = \frac{3-\sqrt{3}}{4\sqrt{2}} \\ c_2 = \frac{3-\sqrt{3}}{4\sqrt{2}} \\ c_3 = \frac{1-\sqrt{3}}{4\sqrt{2}} \end{matrix} \quad (6)$$

$$c_3 - c_2 - c_1 - c_0 = 0 \quad (7) \quad 0 \cdot c_3 - 1 \cdot c_2 + 2 \cdot c_1 - 3 \cdot c_0 = 0 \quad (8)$$

Where, $C^T \cdot C = I$. The first line in Eq. (6) is called scaling coefficients and second line is called wavelets coefficients. Forth Daubechies function (N=4) has four coefficients in a line. The first line shows a transform to obtain a mean value with weights of c_0, c_1, c_2 and c_3 on the input data. The second line shows a transform to obtain a difference value with weights of c_0, c_1, c_2 and c_3 on the input data. The third line shows a transform to translate the first line by two steps. The fourth line is a transform to do the second line by two steps. Eqs. (7) and (8) show the transformed values are zero when the input data are constant or are simply increased. To explain easily the process to acquire the analyzing wavelets matrix W from C , the matrix X is assumed as one dimensional 16 elements,

$$X = [x_1 \ x_2 \ x_3 \ x_4 \ x_5 \ x_6 \ x_7 \ x_8 \ x_9 \ x_{10} \ x_{11} \ x_{12} \ x_{13} \ x_{14} \ x_{15} \ x_{16}]^T \quad (9)$$

From Eqs. (6) and (9), the transformed matrix X' is

$$X' = C_{16} X = [s_1 \ d_1 \ s_2 \ d_2 \ s_3 \ d_3 \ s_4 \ d_4 \ s_5 \ d_5 \ s_6 \ d_6 \ s_7 \ d_7 \ s_8 \ d_8]^T \quad (10)$$

Where, C_{16} is 16X16 matrix of C . The element s indicates the mean value and the element d indicates the difference value. The elements in the matrix X' are replaced by a matrix P_{16} .

$$P_{16} X' = P_{16} C_{16} X = [s_1 \ s_2 \ s_3 \ s_4 \ s_5 \ s_6 \ s_7 \ s_8 \ d_1 \ d_2 \ d_3 \ d_4 \ d_5 \ d_6 \ d_7 \ d_8]^T \quad (11)$$

Where, P_{16} is defined as

$$P_{16} = \begin{pmatrix} 1 & 0 & 0 & 0 & 0 & 0 & 0 & 0 & 0 & 0 & 0 & 0 & 0 & 0 & 0 & 0 \\ 0 & 0 & 1 & 0 & 0 & 0 & 0 & 0 & 0 & 0 & 0 & 0 & 0 & 0 & 0 & 0 \\ 0 & 0 & 0 & 0 & 1 & 0 & 0 & 0 & 0 & 0 & 0 & 0 & 0 & 0 & 0 & 0 \\ 0 & 0 & 0 & 0 & 0 & 0 & 1 & 0 & 0 & 0 & 0 & 0 & 0 & 0 & 0 & 0 \\ 0 & 0 & 0 & 0 & 0 & 0 & 0 & 0 & 1 & 0 & 0 & 0 & 0 & 0 & 0 & 0 \\ 0 & 0 & 0 & 0 & 0 & 0 & 0 & 0 & 0 & 0 & 1 & 0 & 0 & 0 & 0 & 0 \\ 0 & 0 & 0 & 0 & 0 & 0 & 0 & 0 & 0 & 0 & 0 & 0 & 1 & 0 & 0 & 0 \\ 0 & 0 & 0 & 0 & 0 & 0 & 0 & 0 & 0 & 0 & 0 & 0 & 0 & 0 & 1 & 0 \\ 0 & 1 & 0 & 0 & 0 & 0 & 0 & 0 & 0 & 0 & 0 & 0 & 0 & 0 & 0 & 0 \\ 0 & 0 & 1 & 0 & 0 & 0 & 0 & 0 & 0 & 0 & 0 & 0 & 0 & 0 & 0 & 0 \\ 0 & 0 & 0 & 0 & 1 & 0 & 0 & 0 & 0 & 0 & 0 & 0 & 0 & 0 & 0 & 0 \\ 0 & 0 & 0 & 0 & 0 & 0 & 1 & 0 & 0 & 0 & 0 & 0 & 0 & 0 & 0 & 0 \\ 0 & 0 & 0 & 0 & 0 & 0 & 0 & 0 & 1 & 0 & 0 & 0 & 0 & 0 & 0 & 0 \\ 0 & 0 & 0 & 0 & 0 & 0 & 0 & 0 & 0 & 0 & 1 & 0 & 0 & 0 & 0 & 0 \\ 0 & 0 & 0 & 0 & 0 & 0 & 0 & 0 & 0 & 0 & 0 & 0 & 1 & 0 & 0 & 0 \\ 0 & 0 & 0 & 0 & 0 & 0 & 0 & 0 & 0 & 0 & 0 & 0 & 0 & 0 & 1 & 0 \\ 0 & 0 & 0 & 0 & 0 & 0 & 0 & 0 & 0 & 0 & 0 & 0 & 0 & 0 & 0 & 1 \end{pmatrix} \quad (12)$$

Moreover, from Eq. (11), the transform is continuously carried out by C and P without any operations to the difference values,

$$W^{(3)} X = [S_1 \ S_2 \ S_3 \ S_4 \ D_1 \ D_2 \ D_3 \ D_4 \ d_1 \ d_2 \ d_3 \ d_4 \ d_5 \ d_6 \ d_7 \ d_8]^T \quad (13)$$

$$S = W^{(3)} X = [S_1 \ S_2 \ D_1 \ D_2 \ D_3 \ D_4 \ d_1 \ d_2 \ d_3 \ d_4 \ d_5 \ d_6 \ d_7 \ d_8]^T \quad (14)$$

Where,

$$W^{(2)} = (P_{16}^T C_{16}^T) (P_{16} C_{16}) \quad (15)$$

$$W^{(3)} = (P_{16}^T C_{16}^T) (P_{16}^T C_{16}^T) (P_{16} C_{16}) \quad (16)$$

$$P_{16}^T = \begin{bmatrix} P_1 & 0 \\ 0 & I_8 \end{bmatrix}, C_{16}^T = \begin{bmatrix} C_1 & 0 \\ 0 & I_8 \end{bmatrix}, P_{16} = \begin{bmatrix} P_1 & 0 \\ 0 & I_8 \end{bmatrix}, C_{16} = \begin{bmatrix} C_1 & 0 \\ 0 & I_8 \end{bmatrix} \quad (17)$$

$W^{(3)}$ is a analyzing wavelets matrix that is W in Eq. (2). The wavelets spectrum S in Eq. (2) is $W^{(3)} X$ in Eq. (14). In Eq. (13), S_1 indicates the mean value from s_1 to s_4 in Eq. (11). S_2 indicates the mean value from s_5 to s_8 that translate by two steps. D_1 indicates the difference value from s_1 to s_4 . In Eq. (14), S_1 indicates the mean value from S_1 to S_2 in Eq. (13). D_1 indicates the difference value from S_1 to S_2 in Eq. (13). From Eq. (14), the input data are transformed to the mean values and the difference values with valuable resolution levels by the discrete wavelets transform. The input data are divided into a range from high frequency to low frequency. From Eq. (14), the inverse wavelets transform is,

$$X = |W^{(3)}|^T S \quad \text{---(18)}$$

$$|W^{(3)}|^T = [(P_{16}^{(1)} C_{16}^{(1)})^T (P_{16}^{(2)} C_{16}^{(2)})^T (P_{16}^{(3)} C_{16}^{(3)})^T] \\ = C_{16}^{(1)T} P_{16}^{(1)T} (C_{16}^{(2)})^T (P_{16}^{(2)})^T (C_{16}^{(3)})^T (P_{16}^{(3)})^T \quad \text{---(19)}$$

From Eq. (18), the multiresolution is,

$$X = |W^{(3)}|^T S = |W^{(3)}|^T S_0 + |W^{(3)}|^T S_1 + |W^{(3)}|^T S_2 + |W^{(3)}|^T S_3 \quad \text{---(20)}$$

Where,

$$S_0 = [S_1 \ S_2 \ 0 \ 0 \ 0 \ 0 \ 0 \ 0 \ 0 \ 0 \ 0 \ 0 \ 0 \ 0 \ 0 \ 0]^T \\ S_1 = [0 \ 0 \ D_1 \ D_2 \ 0 \ 0 \ 0 \ 0 \ 0 \ 0 \ 0 \ 0 \ 0 \ 0 \ 0]^T \\ S_2 = [0 \ 0 \ 0 \ 0 \ D_1 \ D_2 \ D_3 \ D_4 \ 0 \ 0 \ 0 \ 0 \ 0 \ 0 \ 0]^T \\ S_3 = [0 \ 0 \ 0 \ 0 \ 0 \ 0 \ 0 \ 0 \ d_1 \ d_2 \ d_3 \ d_4 \ d_5 \ d_6 \ d_7 \ d_8]^T \quad \text{---(21)}$$

In the case of sixteen input data and fourth Doubechies, multiresolution indicates from Level 0 to Level 3. In general, in the case that input data is 2^n and Doubechies function is k th ($N=k$), the algorithm to obtain levels is shown in Fig. 1. The final wavelets spectrum is obtained after the wavelet transform in Eq (14) continues until the number of final summation elements is less than k .

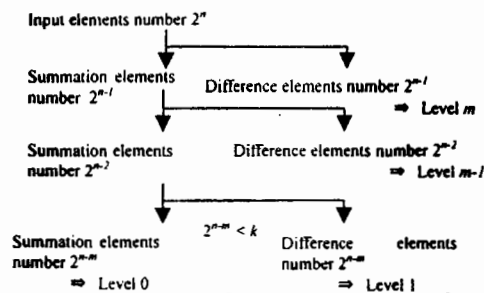


Fig. 1 Algorithm of discrete wavelets transform

EXPERIMENTS

Nozzle to Produce Spiral Flow

The nozzle to produce the spiral flow is designed with an annular slit connecting to a conical cylinder as shown in Fig. 2 [Horii 1988]. Pressurized air is forced through the sides of the device into the buffer area, and then through the annular slit into a vertical pipe entrance. The suction force is generated at the back of the nozzle by Coanda effect. The annular flow, passing through the conical cylinder, develops a spiral structure with a steeper axial velocity and an azimuthal velocity distributions, even if it is not applied tangentially. Vaporized water as a tracer of LDV are sucked into the nozzle from the back of the nozzle. An ejector is used to generate the typical turbulence flow.

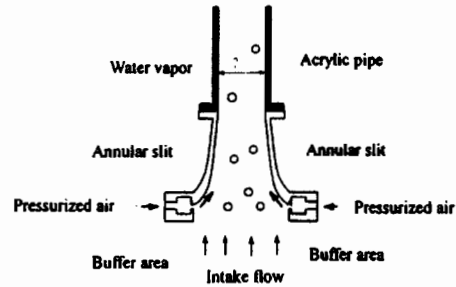


Fig.2 Spiral flow nozzle

Experimental Equipment, Method & Conditions

The experimental equipment consisted of a vertical acrylic pipe, the nozzle to produce the spiral flow and an air compressor as shown in Fig. 3. The inside diameter of the vertical pipe was 41.0 mm. A LDV probe is set up at the side of the vertical pipe at 1.0 m from the air supply part to measure the axial velocity at the center of the pipe. The He-Ne Laser power of LDV was 10 mW, and the probe pick up the reflected wave from the tracer. The air flow rate was $1.98 \times 10^{-3} \text{ m}^3/\text{s}$. The mean velocity of the air flow in the vertical pipe calculated from the flow rate was 1.50 m/s. Reynolds number calculated from the mean velocity was about 4,200.

The reflected wave pass through a timer unit connecting to LDV probe for 1ms (1,000 Hz) pick-up interval. The signals of the reflected wave were counter for about 5 seconds in a counter system connecting to the timer unit. The discrete sampling velocity data were $n=1024 (=2^{10})$. The counter system has high pass and low pass filters that reduce signals under 0.625 m/s and over 6.25 m/s as noise. The pick up point is one point where is the center of the pipe as a first step study. The time mean velocities and turbulence levels of the spiral flow and typical turbulence flow are compared.

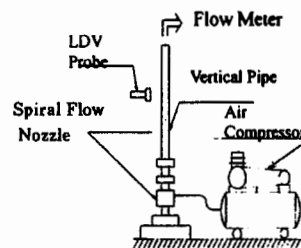


Fig. 3 Experimental equipment

Experimental Results

The velocities of the spiral flow and typical turbulence flow at the center of the pipe are obtained with LDV. The turbulence level is defined as,

$$v' = \frac{1}{n} \sum_{k=1}^n \left[\sqrt{(v_k - v_{mean})^2} / v_{mean} \right] \quad (22)$$

Where, n is the sampling velocity number, v_{mean} is the time mean velocity and v_k is a velocity in a time. The time-mean velocity and the turbulence level are shown in Table 1. From this table, the time mean velocity of the spiral flow is higher than that of typical turbulence flow by about 9 % even though the air flow rate is the same [Horii 1990]. That is because the axial velocity of the spiral flow is steeper than that of the typical turbulence flow. Also, the turbulence level of the spiral flow is much lower than the typical turbulence flow by about 10 %. It means the spiral flow is a stable flow in an axial direction. The normalized axial turbulence velocities $v'_m = (v_m - v_{mean}) / v_{mean}$ are shown in Figs. 4 and 5. These figures are analyzed in the next section.

Table 1 Time-mean velocity and turbulence Level

	Time mean velocity v_{mean}	Turbulence level v'
Spiral Flow	1.93 m/s	0.06616
Typical Turbulence Flow	1.77 m/s	0.07336



Fig. 4 Axial turbulence velocity of spiral flow

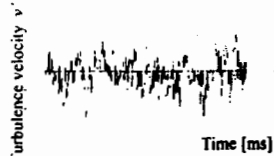


Fig. 5 Axial turbulence velocity of typical turbulence flow

ANALYSIS AND DISCUSSION

Analysis Method

The normalized axial turbulence velocities in Figs. 4 and 5 are analyzed by discrete wavelets transform and its autocorrelation. This wavelet analysis consists of three steps. Firstly, the 1024 ($=2^{10}$) sampling data of the axial turbulence velocities are put into the matrix X in Eq. (9). The matrix X is transformed to the wavelets spectrum S in Eq. (14). Next, the multiresolution analysis is carried out, that is, each part of the spectrum is inversely transformed to multiresolution levels by means of the discrete inverse wavelets transform in Eq. (20). Finally, to recognize which level is dominant for the spiral flow stability, autocorrelation of each level is obtained.

Twentieth Daubechies function is used as an analyzing wavelets function. Twentieth Daubechies function has twenty coefficients from c_0 to c_{20} in the first line in Eq. (6), twenty coefficients from c_{20} to $-c_0$ in the second line in Eq. (6). In the case of twentieth Daubechies function and 1024 ($=2^{10}$) input

data, the multiresolution classifies to seven levels as shown in Eq.(23).

$$X = [W^{(5)}]^T S = [W^{(5)}]^T S_0 + [W^{(5)}]^T S_1 + [W^{(5)}]^T S_2 + [W^{(5)}]^T S_3 + [W^{(5)}]^T S_4 + [W^{(5)}]^T S_5 + [W^{(5)}]^T S_6 \quad (23)$$

$W^{(5)}$ indicates the five times operation to obtain Daubechies matrix from a matrix C in Eq. (6). The coefficients of twentieth Daubechies function are shown in Fig. 6. x axis shows the coefficients from c_{20} to c_0 in the second line of C matrix in Eq. (6). Therefore, 1 in x axis indicates c_{20} , 2 in x axis indicates c_{19} , and 20 indicates c_0 .

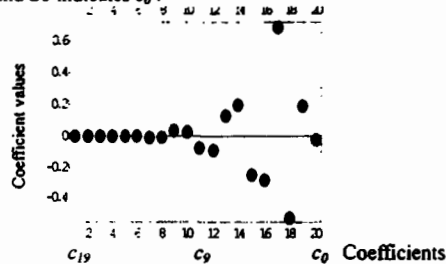


Fig. 6 Coefficients of twentieth Daubechies function

Turbulence Level on Each Frequency Level

To clarify the difference between wavelets transform and Fourier transform, the axial turbulence level on each frequency level defined in Eq. (24) is calculated before indicating the wavelets analysis.

$$v'_m = \frac{1}{n} \sum_{k=1}^n \left[\sqrt{(v'_k - v'_{levelmean})^2} \right] \quad (24)$$

Where, m is a frequency level, $v'_{levelmean}$ is a time mean turbulence velocity and v'_k is a turbulence velocity in a time on each wavelet level. The v'_m indicates a kind of normalized turbulence level obtained by Fourier transform. The mean turbulence velocity on each frequency level $v'_{levelmean}$ is not zero. The turbulence level on each frequency level is shown in Fig. 7 (Level 0 is not shown). From this figure, the turbulence levels of the spiral flow on all levels are lower than those of typical turbulence flow. Mainly, the level from Level 1 to Level 4 are remarkably different. Both turbulence levels have peaks at Level 3.

The relation between the frequency level and the wave number is shown in Table 2. If Kolmogorov wave number k_d is assumed to be 10^1 order, the wave number range normalized with k_d is from 10^0 to 10^{-1} . It means that the range includes the energy contain range and the inertia range. The position of the peaks are reasonable from Kolmogorov theory.

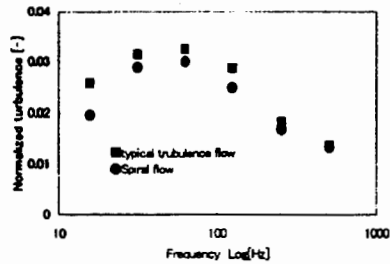


Fig. 7 Turbulence level on each frequency level

Table 2. Relation between Frequency and Wave number

	Level 1	Level 2	Level 3	Level 4	Level 5	Level 6
Wave number	5.1	1.0	2.0	4.1	8.1	1.6
Spiral flow [cm ⁻¹]	X 10 ⁻¹	X 10 ⁰	X 10 ⁰	X 10 ⁰	X 10 ⁰	X 10 ¹
Wave number	5.5	1.1	2.2	4.4	8.9	1.8
Typical flow [cm ⁻¹]	X 10 ⁻¹	X 10 ⁰	X 10 ⁰	X 10 ⁰	X 10 ⁰	X 10 ¹

Wavelets Analysis Results & Discussion

Transforming inversely each level of the wavelets spectrum indicates multiresolution as shown in Eq.(20). Fig. 8(A) shows the multiresolution of the spiral flow, and Fig. 8(B) shows the multiresolution of the typical turbulence flow in three dimension display. From Fig. 8, it is recognized that time and frequency level is simultaneously analyzed. To clarify the each frequency level, Fig.8 is displayed in two dimension as shown in Fig. 9. From this multiresolution, the spectrum can be divided from low frequency level (Level 1) to high frequency level (Level 6). The summation from level 0 to level 6 recovers completely the original turbulence velocities in Figs. 4 and 5 (Level 0 is not shown). In the waveform on the low frequency level (Levels 1 and 2) in the figures, the turbulence velocity of the spiral flow is much smaller than this of the typical turbulence flow. The waveform on the middle frequency levels (Levels 3 and 4) is slightly different, and then, high frequency level is the same.

Next, the autocorrelation on each level in Fig. 9 is obtained to classify which level is dominant in the spiral flow with

$$R(\tau) = \frac{\overline{v'_i(t)v'_i(t+\tau)}}{\sqrt{\overline{v'^2_i(t)}} \cdot \sqrt{\overline{v'^2_i(t+\tau)}}} \quad (25)$$

τ is the delay time from 0.0 to 512 ms. The autocorrelation is done binarization with threshold value +0.25 and -0.25 because the periodicity makes clear. In this study, the points over +0.25 and under -0.25 of the autocorrelation is assumed to be high periodicity, and the points between -0.25 and +0.25 to be low periodicity. The binary autocorrelation is shown in Fig.10. In this figure, the black part is under -0.25, and white part is over +0.25, which are high correlation parts. The gray part is between -0.25 and +0.25, which is low correlation part. From

this figure, it is recognized that Level 3 is dominant in the spiral flow because the black part and the white part are shown repeatedly.

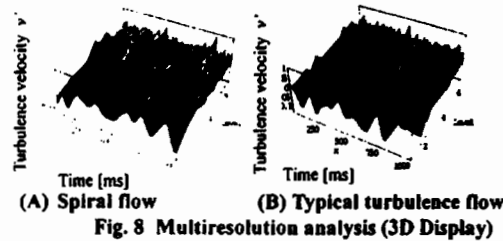


Fig. 8 Multiresolution analysis (3D Display)

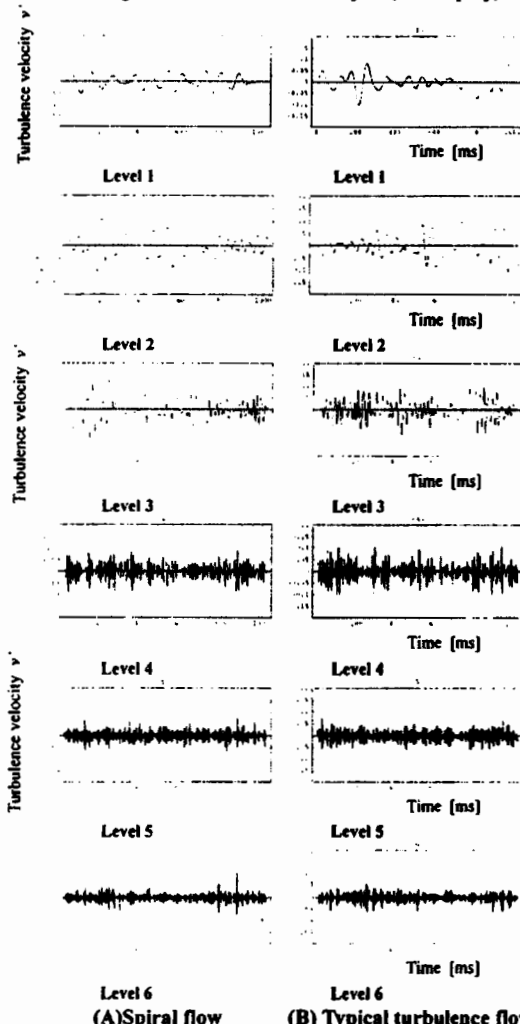
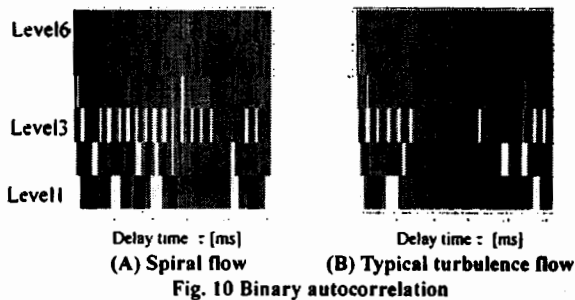


Fig. 9 Multiresolution analysis for turbulence velocity



CONCLUSIONS

Time-frequency distributions of axial turbulence velocities of spiral pipe flow and typical turbulence flow have been clearly decomposed in a range from low frequency level to high frequency level by means of discrete wavelets transform. Also, the dominant level to be stabilized is classified. As a result, the following conclusions become clear.

- (1) The time waveform on target level is able to extract by means of discrete wavelets transform and multiresolution because the orthonormal analyzing wavelets function composes and decomposes the original waveform. It is useful for analyzing the stability of spiral flow
- (2) The axial turbulence level in the under middle frequency levels (under Level 4) of spiral flow are extremely lower as compared with that of typical turbulence flow.
- (3) Level 3 of spiral flow has high periodicity. It means that the axial stability of spiral flow is mainly dominated by Level 3.

ACKNOWLEDGEMENTS

The authors are pleased to acknowledge the considerable assistance of Mr. T. Katayanagi and Mr. K. Kato in Nihon University.

REFERENCES

- Everson, R. and Sirovich, L., (1990) Wavelet Analysis to the Turbulence Jet, *Phys. Lett.*, Vol. 145 No. 6, pp314-322
- Gordeyev, S.V. and Thomas, F.O., (1995) Measurement of Reynolds Stress Reversal in a Planar Jet by Means of a Wavelet Decomposition, *Turbulent Flows ASME FED-Vol. 208*, pp. 49-54
- Horii, K., (1990) Using Spiral Flow for Optical Cord Passing, *Mechanical Engineering - ASME*, Vol. 112, No. 8, pp68-69
- Horii, K. et al., (1991) A Coanda Spiral Device Passing Optical Cords with Mechanical Connectors Attached through a Pipeline, *ASME FED-Vol. 121, Gas-Solid Flows*, pp65-70.
- Horii, K., (1988) *US.PAT. No. 4,721,126, UK.PAT. No. 2, 180, 957*

Li, H. and Nozaki, T., (1995) Wavelet Analysis for the Plane Turbulence Jet (Analysis of large eddy structure), *JSME International Journal Fluids and Thermal Engineering*, Vol. 38, No. 4 pp525-531

Molet, F. et al., (1989) Wavelet Propagation and Sampling Theory, *Geophysics*, Vol. 11

Saito, Y., (1996) Wavelet Analysis for Computational Electromagnetics, (in Japanese), *Trans. IEE of Japan*, Vol. 116A, No. 10, pp833-839

Takei, M. et al., (1997) Transporting Particles without Touching Pipe Wall, *ASME FED. FEDSM97-3629*

Walker, S.H., Gordeyev, S.V. and Thomas, F.O., (1995) A Wavelet Transform Analysis Applied to Unsteady Jet Screech Resonance, *High speed jet flow ASME FED-Vol. 214*, pp103-108